Presented at Workshop on the Analysis of Hydrogen in Solids, Albuquerque, NM January 23-25, 1979. To appear in Proceedings.

SAND79-0210C
Conf. 790107--2

HYDROGEN DEPTH PROFILING USING ELASTIC RECOIL DETECTION*

B. L. Doyle and P. S. Peercy
Sandia Laboratories,† Albuquerque, NM 87185

Abstract

We describe the elastic recoil detection (ERD) analysis technique for H profiling in the near surface regions of solids. ERD is shown to have the capability of detecting H and its isotopes down to concentrations of ~0.01 at.% and with a depth resolution of a few hundred angstroms. We also demonstrate that 2.4 MeV He ions can be used successfully to profile ^{1}H and ^{2}D using this technique.

I. INTRODUCTION

Elastic recoil detection (ERD)[1] is an alternative method to both resonant and nonresonant nuclear reaction analysis (NRA)[2] for nondestructively obtaining H (and other light element) depth profiles in solids. Although for most cases ERD has poorer sensitivity and depth resolution than NRA, there exist many experimental situations where ERD can be considered equal or superior to NRA. In this paper we compare ERD, utilizing several analysis beams, with 6.4 MeV $^{19}F(^{1}H,\alpha\gamma)^{16}O$ resonant NRA. In Section II the ERD experimental arrangement is described, along with a short review of the scattering kinematics and a discussion on the optimization of depth resolution. Section III contains H and other light ion profiles obtained by ERD, and in Section IV we show H and D profiles obtained simultaneously with a 2.4 MeV ^{4}He analysis beam. Section V gives a comparison of ERD and NRA (6.4 MeV $^{19}F(H,\alpha\gamma)^{16}O$) and the advantages and disadvantages of ERD are discussed in the conclusion, Section VI.

II. EXPERIMENTAL ARRANGEMENT

The principle behind ERD is quite simple with the technique being similar to ion backscattering. The scattering geometry is shown schematically in Fig. 1. (A similar recoil method utilizing thin samples and transmitted ion beams will not be discussed.) For ERD, a beam of ions, usually obtained from a tandem accelerator, with mass M_1 greater than that of the atoms to be profiled (M_2) and energy E_{in} ~1 MeV/amu, is incident on a sample tilted at an angle θ_{in} with respect to the incident beam.

*This article sponsored by the U. S. Department of Energy, under Contract AT(29-1)-789.
†A U. S. Department of Energy Facility.

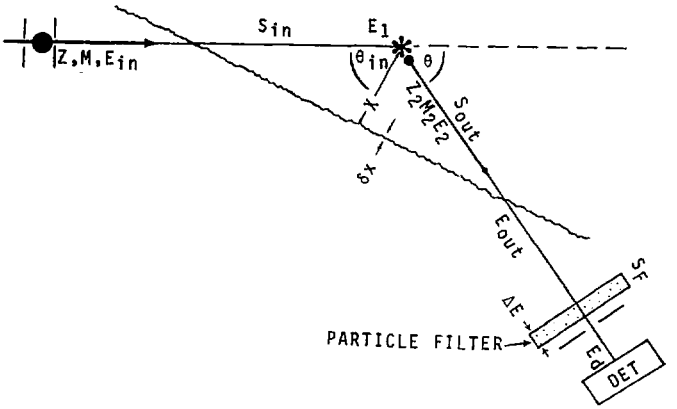

Fig. 1. Elastic recoil detection (ERD) forward scattering geometry using reflection geometry for analysis of thick samples.

The incident beam undergoes elastic collisions with atoms in the target while it decelerates along its trajectory according to the stopping power of the sample, S_{in}. One such collision is depicted in Fig. 1 where at depth x an atom of mass M_2 is recoiled out of the target at an angle θ by the incident ion whose energy has now dropped to E_1. Although the recoiled ion initially has energy E_2, it also loses energy while traversing the target and exits with an energy of E_{out}. The stopping power for this loss of energy is S_{out}.

The recoiled ions are detected by a silicon surface-barrier detector covered by both a collimating slit and a thin foil. The aperture is used for definition of the scattering angle and the foil, called a range foil, acts as a particle filter, transmitting the light recoiling ions from the target but stopping the analysis ions which have been elastically scattered in this same direction. The recoiled ions are detected (for this example) with energy $E_D = E_{out} - \Delta E$ where ΔE is the energy lost in the foil.

For many cases the tilt of the sample θ_{in} is chosen so that the target normal bisects the angle between the incident and recoiled ions (i.e., $\theta_{in} = (\pi - \theta)/2$). If we assume that the stopping

powers S_{in} and S_{out} are constant, the detected energy of the recoiling ion can be expressed as:

$$E_d = KE_{in} - [S]x - \Delta E \tag{1}$$

where

$$[S] = \frac{KS_{in}}{|\cos(\theta_{in})|} + \frac{S_{out}}{|\cos(\theta+\theta_{in})|} \tag{2}$$

and the kinematic factor[3] K is

$$K = \frac{4\ M_1M_2}{(M_1+M_2)^2} \cos^2\ \theta\ . \tag{3}$$

Data are collected in a multichannel fashion for a prescribed number of incident ions and the concentration of recoiled ions previously in the sample is obtained from the equation

$$N(x) = \frac{Y \cdot \frac{dE_d}{dx}}{Q \cdot \frac{d\sigma}{d\Omega}\Delta\Omega \cdot E_c} \tag{4}$$

where N(x) is the concentration (atoms/cm^3) of detected light atoms in the sample at depth x, Q is the total number of ions incident on the target during the experiment, Y is the yield of recoils per channel at energy E_d, E_c is the detected energy window per channel, and $d\sigma/d\Omega$ is the Rutherford differential scattering cross section for the elastic collision which recoils a target ion into the solid angle $\Delta\Omega$ with an angle θ and is given by

$$\frac{d\sigma}{d\Omega} = \left[\frac{Z_1Z_2e^2(M_1+M_2)}{2M_2\ E_1}\right]^2 \frac{1}{\cos^3\theta}\ . \tag{5}$$

In Eq. 5, Z_1 and Z_2 are the atomic numbers of the incident and recoiled ions, respectively, and e is the electron charge. It is convenient to use a standard to determine $(d\sigma/d\Omega)\Delta\Omega$, and scale according to Eq. 4. The depth of the profiled atoms is determined by solving Eq. 1 for x given the detected energy of light ions scattered from the sample's surface.

The derivative dE_d/dx in Eq. 3 is also important in determining the depth resolution, as will be discussed later, and can be written as

$$\frac{dE_d}{dx} = R[S] \ . \tag{6}$$

In Eq. 6, R is the ratio of the recoiled ion's stopping power in the foil at energy E_d and E_{out}, i.e.,

$$R = \frac{S_F(E_d)}{S_F(E_{out})} \ . \tag{7}$$

Using the universal scaling suggested by Ziegler[4] and the empirical H stopping powers tabulated by Anderson and Ziegler,[5] we have calculated R and dE_d/dx for the recoil analysis of ^1H, ^2D and ^3T in a Si sample with beams at 1 MeV/amu. Results of these calculations are shown in Figs. 2 and 3. For both of these figures (as well as for Figs. 4 and 5), $\theta = 30°$, $\theta_{in} = 75°$ and the range foil is 10 μm Aℓ with the exception of the 4 MeV ^4He calculations where a 20 μm Aℓ foil was assumed. This thicker foil is necessary to stop the elastically scattered ^4He.

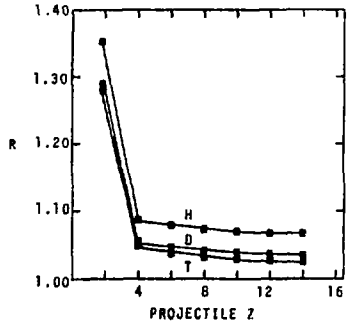

Fig. 2. Effect of range foil on the "stopping power" dE_d/dx for 1 MeV/amu projectiles forward scattering H isotopes from Si samples. $R = S_F(E_d)/S_F(E_{out})$.

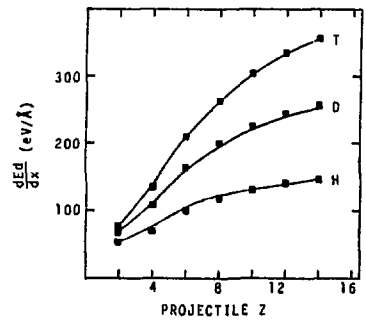

Fig. 3. The "stopping power" dE_d/dx for 1 MeV projectiles recoiling H isotopes from Si.

From Fig. 3, it is clear that the factor R is not very important except for the case of He beams. This result is largely due to the fact that much less energy is imparted to the H in the ^{4}He collisions. Thus, the relative energy loss in the range foil is significantly greater for ^{4}He analysis beams.

The depth resolution for ERD can be expressed as

$$\delta x = \frac{\delta E_d}{dE_d/dx} \tag{8}$$

where δE_d is obtained by the standard error analysis of Eq. 1 and equals:

$$\delta E_d^2 = ([S]\delta x_s)^2 + (E_{in}\delta K)^2 + (\delta \Delta E)^2 + E_r^2 \ . \tag{9}$$

The terms in Eq. 9 correspond to surface roughness, kinematic broadening, straggling and nonuniformity in the range foil and detector resolution, respectively. Terms with smaller contributions have been neglected in Eq. 9.

By examination of Eqs. 6, 8, and 9, it is clear that $\delta x > \delta x_s$. Hence smooth surfaces are a prerequisite for the use of ERD for H profiling. When this condition is met, the kinematic spread term usually dominates, which yields

$$\delta E_d \approx E_{in}\ \delta K \ . \tag{10}$$

It can readily be shown that, for a constant solid angle, δK is minimized when

$$h = 2\sqrt{r \cdot w \cdot \tan\ \theta} \tag{11}$$

where h, w and r are, respectively, the height, width, and distance from sample of the detector aperture. This condition leads to a minimum broadening of

$$\delta K = 3K \tan\ \theta\ \delta\theta \ . \tag{12}$$

Therefore, the depth resolution is proportional to $K/(dE_d/dx)$. This factor is plotted in Fig. 4 as a function of analysis beam and recoiled H isotope.

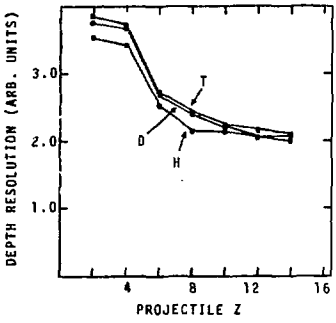

Fig. 4. H depth resolution for 1 MeV/amu projectiles. This figure is valid only if the kinematic broadening term is dominant in Eq. 9.

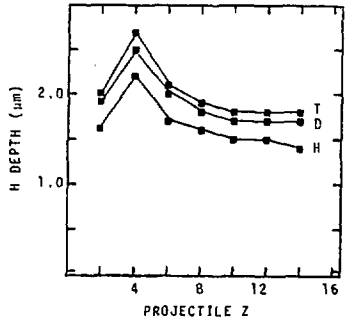

Fig. 5. Maximum depth capabilities of 1 MeV/amu ions in ERD profiling of H isotopes in Si.

A computer program[6] has been developed which iteratively generates the detected recoil energy E_d as a function of target penetration depth (x). Calculations of the maximum depth capability for profiling ^{1}H, ^{2}D and ^{3}T with 1 MeV/amu projectiles are shown graphically in Fig. 5.

III. ERD PROFILING WITH HEAVY ION BEAMS

Until recently, ERD profiles have been obtained exclusively with beams of ~1 MeV/amu heavy ions ranging from ^{16}O to ^{35}C.[1] One of the unique advantages of ERD compared to other ion beam profiling techniques is that multiple light elements can be depth profiled simultaneously with a single analysis beam. This feature is demonstrated in Figs. 6 and 7 where 12 MeV ^{12}C and 24 MeV ^{28}Si beams, respectively, have been used to profile ^{1}H, ^{2}D and ^{4}He implanted into Si. For clarity, only the recoil energy spectrum is shown for the ^{12}C ERD profile (Fig. 6). The depth scales indicated in the Si ERD profile (Fig. 7) were obtained by using the computer program mentioned above.[6] Both yield axes in Figs. 6 and 7 can easily be related to the respective concentrations of ^{1}H, ^{2}D and ^{4}He by use of Eq. 4 if the differential scattering cross sections are assumed constant. For example, the peak concentrations of the ^{1}H, ^{2}D and ^{4}He profiles have been calculated to be 6.1, 6.3, and 5.0 at.%, respectively. Alternatively, the yield in each channel could be adjusted via Eq. 4 to account for the varying cross section and dE_d/dx. The ^{12}C ERD profile depicts two of the potential problems with this technique, namely: (1) ambiguity in the ^{2}D and ^{4}He profiles due to the overlap in

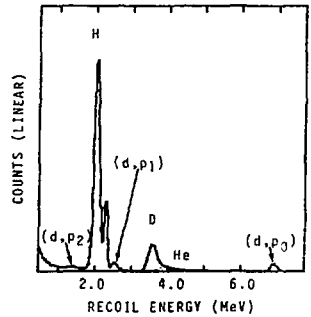

Fig. 6. Recoil energy spectrum of ^{1}H, ^{2}D and ^{4}He which was implanted into Si. The ERD analysis beam was 12 MeV ^{12}C and the peaks resulting from the various target species are indicated in the figure. The double peak for H results from H on the surface as well as implanted H. The three peaks labeled (d,p) indicate $D(^{12}C,p)^{13}C$ nuclear reactions where the ^{13}C residual nucleus is left in its ground state and first two excited states (0, 1 and 2, respectively).

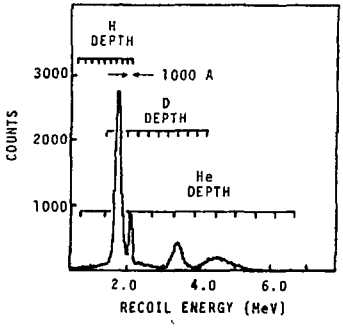

Fig. 7. Recoil spectra for the same sample as in Fig. 6, except that a 24 MeV ^{28}Si analysis beam was used. The depth increments are 1000 Å.

their corresponding energy distributions (~4 MeV) and (2) the possible interference of reaction products caused by inelastic nuclear collisions as shown by the three proton groups labeled in the figure. Both problems can be solved by either using a different analysis beam, as demonstrated by the ^{28}Si ERD profile in Fig. 7, or by use of an E-ΔE particle detector telescope which is capable of detecting not only the ion energy but also the ion mass.

The C ERD H profile in Fig. 8 shows the variation of H in a Si_3N_4-$Si_xO_yN_z$-Si_3N_4 structured sample. During the intermediate period of the sample's growth, 1000 ppm O_2 was introduced in the N_2 carrier gas producing the observed drop in H concentration in this region.

The best combined depth resolution and H sensitivity which we

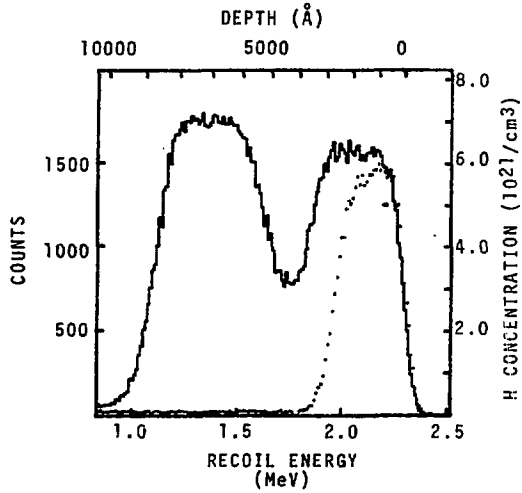

Fig. 8. ERD (12 MeV ^{12}C) profile of ^{1}H in Si_3N_4. The dip at 4000 Å corresponds to the introduction of small amounts of O_2 into the reactor during growth. The dotted curve is the ^{1}H profile of a Si_3N_4 reference sample.

have obtained to date has been 300 Å FWHM at a sensitivity of ~0.01 at.% H using a 24 MeV ^{28}Si beam. In principle, one can trade off resolution for sensitivity and vice versa; however, the best resolution obtainable seems to be ~100 Å.[1] The sensitivity is highly dependent on the amount of surface H on the sample as the observed backgrounds are most likely caused by the secondary scattering of these surface atoms. Surface H contamination is therefore a more serious limitation for ERD than for NRA.

IV. ERD PROFILING WITH LOW ENERGY He BEAMS

One of the most important developments in ERD technology is the recent discovery that low energy He ions can be used to obtain profiles of ^{1}H, ^{2}D and (in principle) ^{3}T in the near surface region of solids.[7] Whereas profiles of ^{2}D and ^{3}T can be readily measured with a Van de Graaff or other low energy particle accelerator,[8,9] sensitive, nondestructive, profiling of ^{1}H has been essentially limited to laboratories having tandem Van de Graaff accelerators.[10] This new ERD technique therefore gives

^{1}H profiling capabilities to facilities having low energy Van de Graaff accelerators commonly used for ion backscattering analysis.

Two ERD profiles using a 2.4 MeV ^{4}He analysis beam are shown in Fig. 9. For the top profile ^{1}H and ^{2}D are present in only the first few hundred angstroms of a Si sample and the resulting profiles of ^{1}H and ^{2}D are clearly represented. The bottom profile, on the other hand, shows what happens when both the ^{1}H and ^{2}D are injected to depths $\geq$3000 A. In this case, an overlap of the resulting energy spectra of ^{1}H and ^{2}D ions occurs, which complicates the analysis. The two spectra were separated in this case by also profiling a sample implanted with ^{1}H only, as shown in the figure. The difference spectrum between the two lower profiles yields the ^{2}D profile shown in Fig. 10. The concentration scale in Fig. 10 is an overestimate because Rutherford cross sections were assumed.

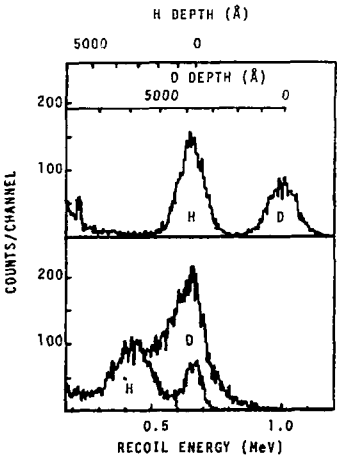

Fig. 9. ERD (2.4 MeV ^{4}He) of ^{1}H and ^{2}D in Si samples. For the top profile both the ^{1}H and ^{2}D are very close to the surface (~100 Å) whereas for the bottom spectrum the ^{1}H and ^{2}D were implanted to a depth of a few thousand angstroms. The profile labeled H resulted from a ^{1}H implant alone.

In Fig. 11 we compare 2.4 MeV ^{4}He ERD with 12 MeV ^{12}C ERD profiles of ^{1}H implanted into Si. The ordinate of this plot corresponds to the count rate at which the data are collected for equal particle currents on target. This figure also shows that the resolution of the ^{4}He ERD profile is ~two times poorer than for the ^{12}C ERD profile.

The optimum H depth resolution and H sensitivity we have obtained

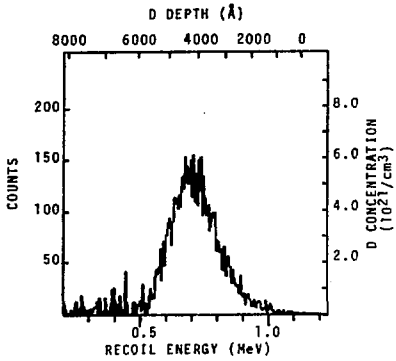

Fig. 10. This spectrum is the difference profile between the two lower curves in Fig. 9 and hence shows the concentration of only ^{2}D as a function of depth.

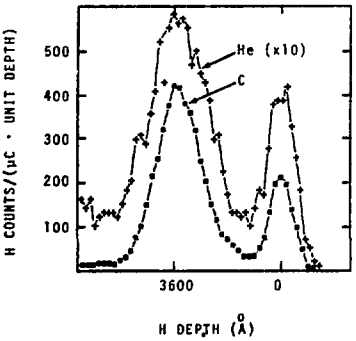

Fig. 11. Comparison of 2.4 MeV ^{4}He ERD with 12 MeV ^{12}C ERD ^{1}H profiling. The ordinate of this plot corresponds closely with data collection rate. The sample was ^{1}H implanted Si.

for ^{4}He ERD are ~700 Å FWHM and 0.1 at.%, respectively. Although these values are poorer than those obtainable by high energy-heavy ion analysis beams, and much poorer than resonant NRA, ^{4}He ERD is quite adequate for many applications. For example, Wampler, et al.,[11] have been using this technique to examine ^{1}H and ^{2}D in Si samples exposed to single discharges of PLT. In fact, the top spectrum in Fig. 9 is one such profile.

V. COMPARISON OF ERD AND NRA

In Fig. 12 we plot profiles of ^{1}H in Si_3N_4 grown at 900°C which were obtained by ^{12}C and ^{4}He ERD in addition to 6.4 MeV

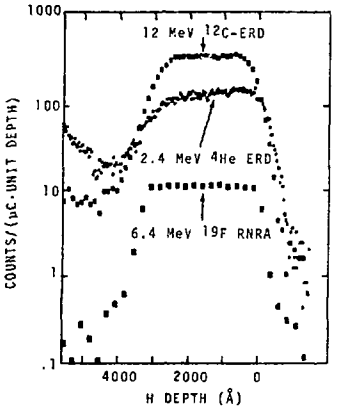

Fig. 12. Comparison of ^{12}C and ^{4}He ERD with 6.4 MeV ^{19}F resonant NRA (RNRA). The sample was CVD Si_3N_4 (~6 at.% ^{1}H) grown at 900°C on Si.

$^{19}F(p,\alpha\gamma)^{16}O$ resonant NRA (called RNRA in the figure). This plot is similar to that of Fig. 11, in that it depicts count rate, except in this case the graph is semilogrithmic.

The resonant NRA profile is somewhat deceiving as presented in Fig. 12. Since the points are taken one-at-a-time, the total integrated charge on target is much larger than that necessary to obtain just one point. This means that although the actual counting rate per channel of 6.4 MeV ^{19}F resonant NRA is quite comparable to that of ^{12}C ERD, when one considers the number of data points necessary to obtain the complete profile, the profiles are obtained in a much slower fashion. This figure indicates that the fastest method for obtaining a H profile is by ^{12}C or higher mass ERD.

VI. CONCLUSIONS

In summary, we have described the elastic recoil detection (ERD) technique for obtaining ^{1}H (and its isotopes) depth profiles in the near surface region of solids. While ERD has poorer H depth resolution and sensitivity than does resonant nuclear reaction analysis and requires smooth sample surfaces, it offers such advantages as: (1) increased data collection rate (which also corresponds to decreased beam heating and damage to the sample), (2) less complicated experimental procedures (i.e., the analysis beam is operated at fixed energy and contributions at all depths are detected simultaneously), (3) ^{1}H, ^{2}D and ^{3}T are all detectable with the same beam; hence profiles for all H isotopes are

measured in one run and, perhaps most important, (4) H profiling measurements can be performed in a low energy accelerator laboratory using the same instrumentation currently used for ion backscattering analysis.

References

1. B. Terreault, J. G. Martel, R. G. St.-Jacques, and J. L'Ecuyer, J. Vac. Sci. Technol. 14, 492 (1977).
2. J. F. Ziegler, et al., Nucl. Instrum. Methods 149, 19 (1978).
3. J. B. Marion and F. C. Young, "Nuclear Reaction Analysis," (North-Holland-Amsterdam, 1968), p. 142.
4. J. F. Ziegler, Appl. Phys. Lett. 31, 544 (1977).
5. H. H. Anderson and J. F. Ziegler, "Hydrogen Stopping Powers and Ranges in All Elements," (Pergamon Press, New York, 1977).
6. Computer Code ERDANA1 by B. L. Doyle (unpublished).
7. B. L. Doyle and P. S. Peercy (submitted for publication).
8. See Refs. 5 and 10 (loc. cit. 2).
9. J. C. Davis and J. D. Anderson, J. Vac. Sci. Technol. 12, 358 (1975).
10. The H(^{11}B,γ) resonant NRA technique uses low energy Van de Graaffs but has poor sensitivity and resolution; see Ref. 4 (loc. cit. 2).
11. W. R. Wampler, S. T. Picraux, S. A. Cohen, H. F. Dylla, G. M. McCraken, S. Rossnagle, L. W. Magee, J. Nucl. Mater. (submitted for publication).